Interaction of the Atlantic Equatorial Cold Tongue and the African Monsoon*

YUKO OKUMURA

Department of Meteorology, University of Hawaii at Manoa, Honolulu, Hawaii

SHANG-PING XIE

International Pacific Research Center, and Department of Meteorology, University of Hawaii at Manoa, Honolulu, Hawaii

(Manuscript received 26 September 2003, in final form 18 January 2004)

ABSTRACT

The seasonal cycle of equatorial Atlantic sea surface temperature (SST) is characterized by a rapid cooling from April to July, coinciding with the onset of the West African summer monsoon and followed by a slow warming that lasts 3 times longer. Two ensemble simulations are carried out with an atmospheric general circulation model to investigate the mechanisms for the wind changes that cause this rapid oceanic cooling and its feedback onto the African monsoon. In the control simulation, SST is globally prescribed in its full climatological seasonal cycle, while in the second simulation, equatorial Atlantic SST is held constant in time from 15 April onward.

Comparison of these simulations indicates that the equatorial cooling exerts a significant influence on the African monsoon, intensifying the southerly winds in the Gulf of Guinea and pushing the continental rainband inland away from the Guinean coast. The intensification of the cross-equatorial southerlies associated with the onset of the African monsoon, in turn, triggers the oceanic cooling in the east. The equatorial easterlies are also important for the seasonal cooling by inducing local upwelling and raising the thermocline in the east.

Three mechanisms are identified for the easterly wind acceleration in the equatorial Atlantic in boreal summer. First, the monsoon rainfall distribution is such that it induces zonal sea level pressure gradients and easterly anomalies in the eastern Atlantic. Second, the strong cross-equatorial southerlies advect the easterly momentum from the south into the equator. Finally, zonal pressure gradients associated with the equatorial ocean cooling accelerate surface easterly winds in the middle and western Atlantic. This interaction of equatorial SST and zonal wind causes their westward copropagation, analogous to that in the equatorial Pacific.

1. Introduction

On the equator, insolation at the top of the atmosphere displays small seasonal variations, with a semiannual cycle of 18 W m^{-2} in amplitude exceeding the annual cycle by 23%. However, the equatorial eastern Pacific and Atlantic exhibit a pronounced annual cycle in sea surface temperature (SST), surface wind, and deep convective activity (Mitchell and Wallace 1992). In both equatorial oceans, SSTs reach their maxima in spring when the intertropical convergence zone (ITCZ) comes near the equator. (In this paper, the seasons refer to those for the Northern Hemisphere.) With the onset of the summer monsoon over Central America and West Africa in May–June, the oceanic ITCZ shifts northward over the eastern Pacific and Atlantic, with cross-equatorial southerlies intensifying and the equatorial cold tongue developing rapidly (Fig. 1). The cold tongue reaches its peak in July–August and August–September in the Atlantic and eastern Pacific, respectively. These equatorial oceans then warm up until March. The seasonal evolution of the ITCZ–cold tongue complex in the Atlantic and Pacific is so robust that Mitchell and Wallace (1992) propose that the onset of northern summer monsoons is instrumental in initiating equatorial cooling, and the positive feedback between ocean and atmosphere plays an important role in its intensification and westward expansion.

Xie (1994) proposes that without direct annual forcing from the sun, the climatic asymmetry with respect to the equator—most notably the northward-displaced ITCZ—is the ultimate cause of the equatorial annual cycle in the eastern Pacific and Atlantic (see also Chang 1996). Because of this climatic asymmetry, surface winds are southerly year-round at the equator, strengthening in summer and weakening in spring in response to the seasonal march of the sun. The strengthening

* International Pacific Research Center Contribution Number 273 and School of Ocean and Earth Science and Technology Contribution Number 6369.

Corresponding author address: Yuko Okumura, Department of Meteorology, HIG350, University of Hawaii at Manoa, 2525 Correa Rd., Honolulu, HI 96822.
E-mail: yukoo@hawaii.edu

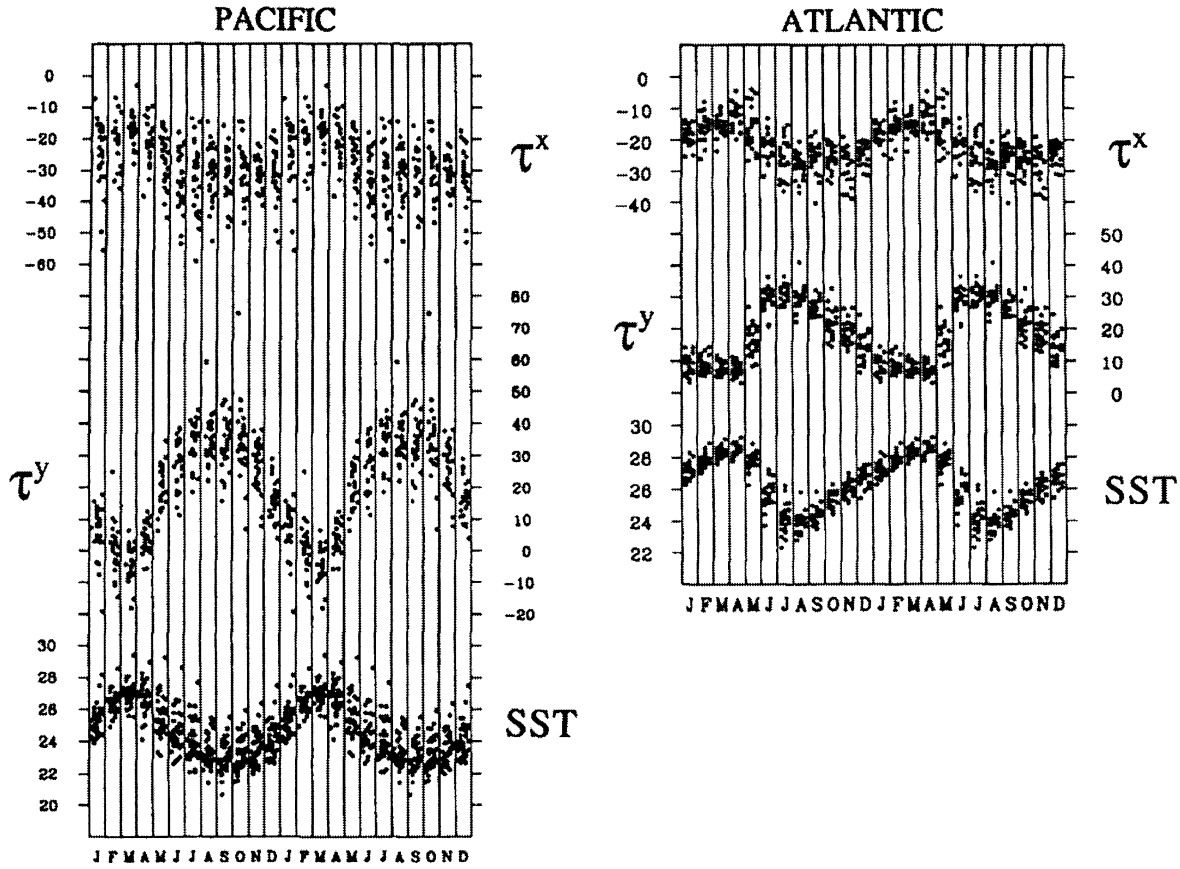

FIG. 1. (a) Scatter diagram of the observed zonal wind stress to the west (4°N–4°S, 130°–110°W), the meridional wind stress to the north (8°N–0°, 120°–100°W) of the Pacific cold tongue, and the cold tongue SST (°C; 4°N–4°S, 104°–86°W). (b) As in (a), but for the zonal wind stress in the western equatorial Atlantic (4°N–4°S, 34°–26°W), the meridional wind stress in the Gulf of Guinea (6°N–0°, 16°W–4°E), and the cold tongue SST (4°N–4°S, 16°W–4°E). Adopted from Mitchell and Wallace (1992).

(weakening) of these southerlies lowers (raises) equatorial SST in summer (spring) by enhancing (reducing) the vertical mixing, surface evaporation (Xie 1994), and upwelling[1] (Philander and Pacanowski 1981). Such southerly wind-induced changes in SST are greatest in the eastern ocean where the thermocline is shallow. The resultant anomalous SST gradients intensify (weaken) the equatorial easterly winds in summer (spring). Displaced west of the maximum SST changes, the easterly wind acceleration helps to propagate the coupled SST–wind anomalies westward through upwelling and evaporation (Mitchell and Wallace 1992; Xie 1994; Nigam and Chao 1996). With regard to the origin of the northward displacement of the ITCZ, continental asymmetry, such as the bulge of western Africa for the Atlantic and the northwest orientation of the Pacific coast of the Americas for the Pacific, is the trigger (Philander et al. 1996), with positive feedback between the ocean and atmosphere helping sustain the climatic asymmetry far away from the coast into the west (see Xie 2004 for a recent review).

While the seasonal warming and cooling are roughly symmetric in their durations in the eastern equatorial Pacific, they are highly asymmetric in the Atlantic, where the cooling takes only three months to reach the peak but takes 3 times longer to warm up (Fig. 1). The tropical Atlantic, with a narrow basin, is strongly influenced by the major continents on both sides. Li and Philander (1997) suggest that the annual cycle in the eastern equatorial Atlantic is largely a passive response to continental monsoons through their effect on oceanic winds, with local air–sea interaction playing a minor role. Comparing to a control simulation forced by seasonally varying SST, their atmospheric general circulation model (AGCM), with annual mean SST prescribed globally, reproduces the seasonal cycle in the meridional (zonal) wind component over the eastern (western) equatorial Atlantic. In the equatorial Pacific, by contrast, they report a substantial reduction in equatorial wind variations, confirming that they result from

[1] Near the equator, surface ocean currents flow downwind, while they become perpendicular to the wind direction 2°–3° away from the equator due to the Coriolis effect. Because of this change in flow regimes, cross-equatorial southerly winds generate ocean upwelling south and downwelling north of the equator.

interaction with the ocean. Li and Philander's result that the annual cycle in equatorial Atlantic SST has little effect on equatorial winds is rather surprising and needs to be reconciled with the observed westward copropagation of equatorial SST and zonal wind, a trait of the equatorial annual cycle that is thought of as indicative of their interaction (Mitchell and Wallace 1992; Xie 1994; Nigam and Chao 1996). While it is easy to understand the forcing of cross-equatorial wind variations by the West African monsoon, it is rather unclear, and these authors did not discuss, how continental monsoons might force an annual cycle in equatorial zonal wind in the western Atlantic.

Whereas the African monsoon's effect on the seasonal cooling of the equatorial Atlantic is well established in the literature, the latter's effect on the monsoon has not been investigated. Results from studies of interannual variability offer some hint of this cold tongue–monsoon interaction on the seasonal time scale. The Atlantic cold tongue displays significant year-to-year variations in strength, with an equatorially trapped anomaly pattern akin to the ENSO in the Pacific (Zebiak 1993). It has been suggested that these SST anomalies are well correlated with summer rainfall in the Sahel and the coastal region facing the Gulf of Guinea (e.g., Lamb 1978; Hastenrath 1984; Lough 1986; Janowiak 1988; Wagner and da Silva 1994). When the eastern equatorial Atlantic SST is anomalously warm, rainfall tends to be below normal over the Sahel and above normal along the Guinean coast, resulting in a meridional dipole of precipitation anomalies over West Africa. More recent studies using longer data records confirm these findings (Janicot et al. 1998; Ward 1998; Fontaine et al. 1999). Eltahir and Gong (1996) show that the West African monsoon intensity and hence the northward penetration of the summer rainband depend upon the meridional gradient of moist static energy in the boundary layer between the Gulf of Guinea and the continent, which is influenced by Atlantic SSTs. Furthermore, Hastenrath (1984) relates much of tropical Atlantic interannual variability to an amplification or phase change of the annual excursion of the ITCZ. Thus, the African monsoon may interact with, instead of exerting one-way influence on, the equatorial annual cycle.

The present study investigates the role of air–sea interaction in the equatorial annual cycle and explores its interaction with the African monsoon by using an AGCM. Our results show that the African monsoon is indeed the major cause of the rapid seasonal cooling in the eastern equatorial Atlantic, but that the subsequent ocean–atmosphere interaction is indispensable for a realistic simulation of the seasonal variations in the monsoon–cold tongue complex. We also identify the mechanisms for the annual cycle in equatorial zonal winds that aid the rapid seasonal ocean cooling. Based on these results, we present a conceptual model for the monsoon–cold tongue interaction on the seasonal time scale. These results may help us understand the source of systematic errors that many state-of-the-art coupled GCMs suffer (Davey et al. 2002). A better understanding of the annual cycle also has important implications for the study of climate variability, which displays a strong seasonality.

The rest of this paper is organized as follows: Section 2 introduces the AGCM used in this study and describes the experimental design. In section 3, the simulated seasonal cycle is compared with observations. Sections 4 and 5 present the results from the model experiments and investigate the monsoon–cold tongue interaction and the seasonal cycle in equatorial zonal winds, respectively. Section 6 includes a summary and discussion.

2. Model and experiment

The atmospheric model used in this study is a global spectral GCM developed jointly by the Center for Climate System Research (CCSR) at the University of Tokyo and the National Institute for Environmental Studies (NIES) in Japan. The CCSR/NIES AGCM 5.6 is widely used as a Japanese community model and is currently being run on the Japan Agency for Marine–Earth Science and Technology's Earth Simulator at very high resolutions. The model consists of the primitive equations and a comprehensive physical package including dry and moist convection, cloud–radiation interaction, turbulence mixing, and land hydrology. Over land, surface albedo is specified and the model forecasts surface temperature and soil moisture. Over the oceans, observed SST is prescribed. Refer to Numaguti et al. (1995) and Numaguti (1999) for model details and performance. We use a version with triangular truncation at zonal wavenumber 42 (T42) and 23 sigma levels in the vertical. Forced with realistic boundary conditions, the model simulates the observed seasonal cycle of the African monsoon fairly well, with some deficiencies that will be discussed in the next section. This model has also been used to successfully simulate the atmospheric response to cross-equatorial SST gradient anomalies in the Atlantic, including the meridional shift of the ITCZ and changes in the trade winds (Okumura et al. 2001).

We conduct two sets of ensemble simulations. In the control (CTL) run, monthly mean climatological SSTs are prescribed globally. Daily values of SST are obtained by linearly interpolating the monthly mean values. In the second set of simulations, we hold equatorial Atlantic SST to its April value from 15 April onward (APR run). In this run, the seasonal cycle of equatorial SST is removed by using a Gaussian weight function centered on the equator with an *e*-folding scale of 10° in latitude. Namely, from 15 April onward, Atlantic SST (T) at latitude ϕ is modified as

$$T = T^* + (T_{\mathrm{Apr}} - T^*) \exp\left[-\left(\frac{\phi}{10}\right)^2\right], \qquad (1)$$

where T^* is the observed SST at a given month and

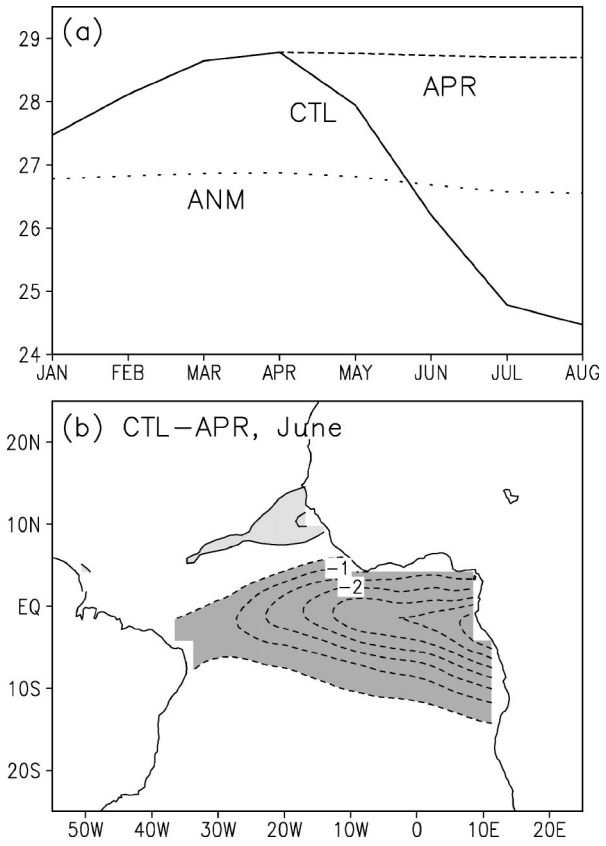

FIG. 2. (a) Seasonal cycle of the equatorial Atlantic SST (°C) in the CTL (solid), APR (dashed), and ANM (dotted) runs, averaged zonally across the basin at 1.4°N/S. (b) CTL − APR SST difference in Jun (light shade > 0.5°C and dark shade < -0.5°C with contours at intervals of 0.5°C).

T_{Apr} is the April value. About 22% (63%) of the seasonal cycle in SST is retained at 5°N/S (10°N/S). Equation (1) successfully suppresses the seasonal development of the cold tongue near the equator, where the annual harmonic of SST reaches a local maximum, without distorting the seasonal cycle off the equator. An additional set of simulations is carried out by forcing the model with annual mean SST in the equatorial Atlantic (ANM run). In the ANM run, the *e*-folding scale is 5°. Figure 2a shows the seasonal cycle of the equatorial Atlantic SST in these experiments. From April onward, SST at 1.4°N/S (the model grid points closest to the equator) remains nearly constant in the APR and ANM runs at 28.8° and 26.8°C, respectively, in contrast to a sharp decrease in the CTL run. Figure 2b shows CTL − APR SST differences in June. The APR run nearly eliminates the equatorial cold tongue.

Li and Philander (1997) specify annual mean SSTs over the entire globe in their sensitivity experiment, which removes not only the equatorial SST annual cycle but also off-equatorial seasonal changes forced directly by the annual march of the sun. After the spring equinox, seasonal changes in insolation warm (cool) the SST north (south) of the equator, and this antisymmetric seasonal cycle of SST contributes to the intensification of the cross-equatorial southerlies (oceanic monsoon) and hence the equatorial cooling. With the purpose of investigating the air–sea interaction along the equator, we choose to suppress the seasonal cycle of SST only in the equatorial Atlantic. Thus, both continental and oceanic monsoons are retained to drive cross-equatorial winds.

The effect of equatorial cold tongue–atmosphere interaction is not limited to the equatorial region but extends along the west coast of Africa to as far south as the Angolan coast by the mechanisms of equatorial and coastal Kelvin waves (e.g., McCreary et al. 1984). Our mask for the equatorial seasonal cycle, Eq. (1), does not remove this remote response in the subtropical Angolan coast (Fig. 2b). This remote response probably has only a limited effect on the atmosphere in the equatorial region given that coastal SSTs are well below the convective threshold.

For the CTL and ANM runs, the model is integrated for 10 yr. The APR run consists of an ensemble of 10 integrations, where each integration is initialized on 1 January using data from the CTL run and lasts until 30 August. Such an ensemble simulation approach allows us to construct a model seasonal cycle that is nearly free of the internal variability of the atmosphere. In the following sections, discussions are made only on those results that are statistically significant at the 95% level based on a Student's *t* test.

3. Simulation of the equatorial seasonal cycle

In the equatorial Atlantic, the first transition from the warm to cold season takes place during April–June in response to the northward migration of the sun. Figures 3a and 3b show changes in surface wind and precipitation from April to June in the CTL run and observations, respectively. In both the model and observations, the center of continental convection moves from the equatorial belt to the Northern Hemisphere over western and central Africa. The northward penetration of the rainband provides a vital source of water for the Sahel region. The anomalous rainbands extend westward across the ocean basin, where they are associated with the northward shift of the oceanic ITCZ. Both over the ocean and Africa, southerly winds feed into the intensifying Northern Hemisphere monsoon across the equator. These enhanced cross-equatorial southerlies cool down the equatorial Atlantic through upwelling, entrainment, and evaporation. While the CCSR/NIES AGCM successfully simulates many of these important features of the seasonal transition, the oceanic ITCZ is considerably weaker, and the spring rainfall over central Africa is too pronounced in the model. The simulated surface wind changes are stronger overall than in observations, and these wind biases stand out especially in the Gulf of Guinea, off the coast of northwest Africa

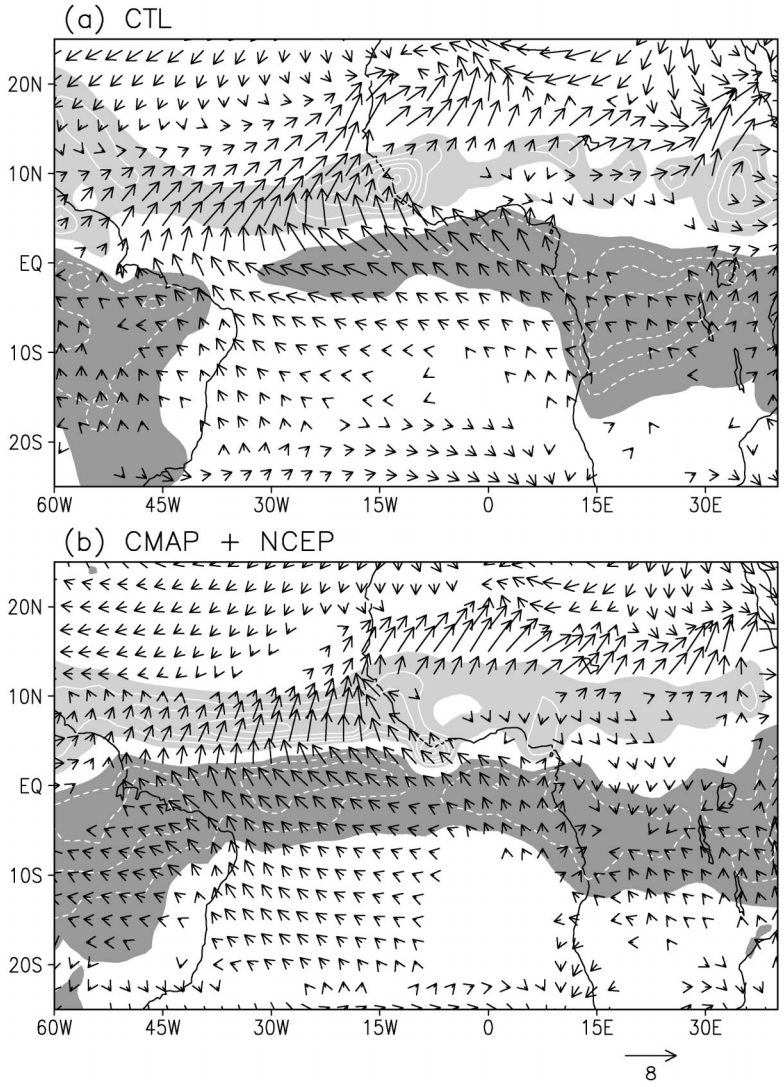

FIG. 3. (a) Jun − Apr changes in precipitation (light shade > 2.0 mm day^{-1} and dark shade < -2.0 mm day^{-1} with white contours at intervals of 2 mm day^{-1}) and surface wind (vectors; m s^{-1}) in the CTL run. (b) As in (a), but for the observed climatology based on the Climate Prediction Center (CPC) Merged Analysis of Precipitation (CMAP; Xie and Arkin 1996) for 1979–2001 and the National Centers for Environmental Prediction–National Center for Atmospheric Research (NCEP–NCAR) surface wind reanalysis (Kalnay et al. 1996) for 1948–2001.

(around 15°N), and the central Atlantic slightly north of the equator.

Besides meridional winds, equatorial zonal winds also play an important role in modulating equatorial SSTs through upwelling, thermocline displacement, and surface heat flux. Figures 4a and 4b show the seasonal cycle of surface zonal wind velocity along the equator in the CTL run and observations based on the Comprehensive Ocean–Atmosphere Data Set (COADS), respectively. Easterly winds prevail over most of the basin, strengthening (weakening) in summer (spring) in association with the expansion (retreat) of the cold tongue. In the model, the zonal winds tend to be too strong, with too large a seasonal range (4–5 m s^{-1}) compared to observations (2–3 m s^{-1}; also see Fig. 11, top). While the observed equatorial winds are easterly west of 5°W throughout a year, the simulated winds turn into westerlies over the eastern half of the basin in winter and spring, consistent with the excessive rainfall over central Africa in those seasons in the model (Fig. 3). As a result, the annual mean equatorial winds in the model have a westerly bias that amounts to 1 m s^{-1} in the east (Fig. 4c). Many other AGCMs appear to have similar problems of westerly bias and excessive continental rainfall (Gates et al. 1999), which may partly explain why many coupled GCMs fail to simulate the

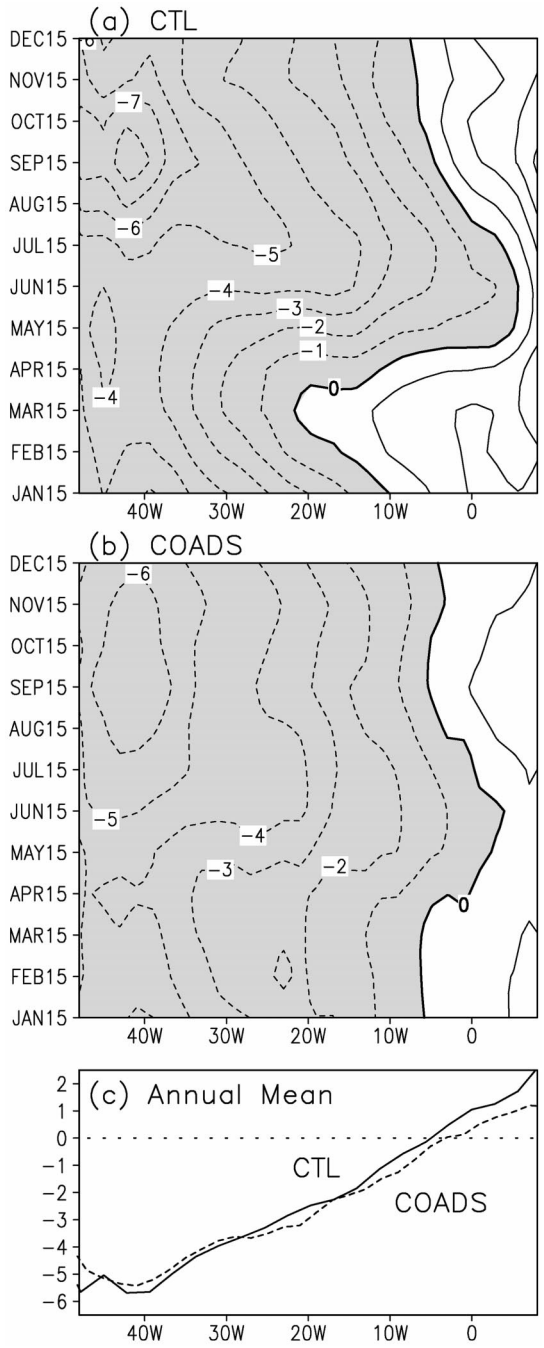

FIG. 4. (a) Seasonal cycle of surface zonal wind velocity (m s^{-1}) along the equator (1.4°N–1.4°S) in the CTL run. Contour intervals are 1.0 m s^{-1} and negative values are shaded. (b) As in (a), but based on the COADS climatology (1.0°N–1.0°S). (c) Annual mean surface zonal wind at the equator in the CTL run (solid) and COADS (dashed).

Atlantic cold tongue (Davey et al. 2002). Despite these biases, the model captures the gross features of the seasonal variations over the equatorial Atlantic and the surrounding continents. The rest of the paper analyzes the model output for a better understanding of mechanisms that shape the seasonal cycle there.

4. Monsoon–cold tongue interaction in the seasonal cycle

With the onset of the West African monsoon in May–June,[2] northward surface winds increase dramatically over the Gulf of Guinea (Fig. 1). The CCSR/NIES AGCM successfully simulates this abrupt onset of summer monsoon when monthly climatological SSTs are prescribed (Fig. 5a). The southerlies start to intensify rapidly in May and continue to strengthen through June concurrently with the development of the cold tongue on the equator. This feature of the African monsoon is very robust and shows little year-to-year variability in the model under the climatological SST forcing.

a. Effect on the African monsoon

The removal of the equatorial cooling in the APR run drastically changes the development of the southerly monsoon over the Gulf of Guinea. The rate of increase in southerly wind speed reduces to half of that in the CTL run (Figs. 5b,c). Figure 6a displays the CTL − APR differences in precipitation and surface winds in June. In the APR run, the ITCZ tends to stay near the Guinean coastal region and the Sahel region receives less rainfall than in the CTL run. The rainfall anomalies are not confined to the eastern Atlantic, where large SST anomalies are present (Fig. 2b), but extend into West Africa to the north and across the basin to South America. In the CTL run, seasonal cooling of the equatorial SST enhances northward gradients of temperature and moist static energy in the atmospheric boundary layer, which are the fundamental forcing of monsoons. As a result, the monsoon rainfall penetrates farther north over West Africa than in the APR run. There are anomalous ascending (descending) motions over the positive (negative) precipitation anomalies throughout the entire troposphere (not shown), as suggested by anomalous surface wind convergence (divergence; Fig. 6a). This north–south dipole pattern of precipitation anomalies has a close resemblance to the observed interannual anomalies associated with the Atlantic Niño over West Africa (Janowiak 1988). In the latitude–time section of the precipitation anomalies (Fig. 6b), this seasonal dipole pattern starts to show up as early as the beginning of May, when the CTL − APR SST anomalies are still modest, and continues to amplify until August, when the cold tongue is fully developed in the CTL run's SST. The node of the precipitation dipole appears to move slowly to the north with the main rainband in the total field. These results indicate that the seasonal development of the Atlantic cold tongue has a significant influence on the development of the African monsoon both on the Guinea coast and in the Sahel.

[2] Here, the monsoon onset is loosely referred to as the rapid intensification of the southerlies in the Gulf of Guinea. There are other definitions of West African monsoon onset (e.g., Sultan and Janicot 2003).

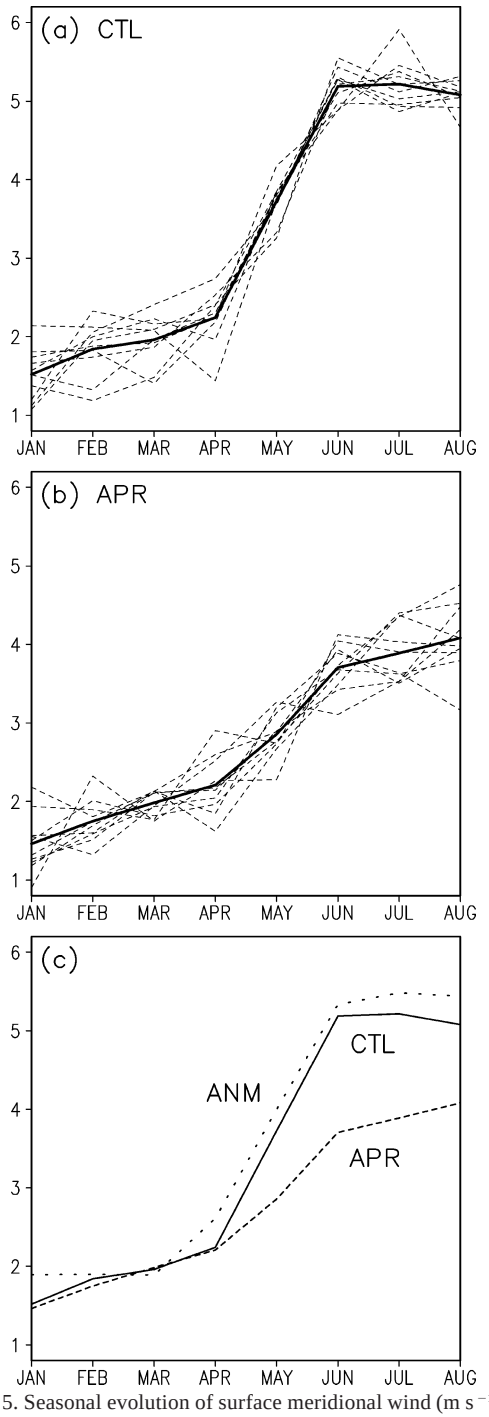

FIG. 5. Seasonal evolution of surface meridional wind (m s^{-1}) over the Gulf of Guinea (1.4°S–4.2°N, 16°W–4°E) in the (a) CTL and (b) APR runs. Dashed lines represent each year of the 10-yr ensemble simulations, and thick solid lines represent the ensemble means. (c) Comparison of ensemble means for the CTL (solid), APR (dashed), and ANM (dotted) runs.

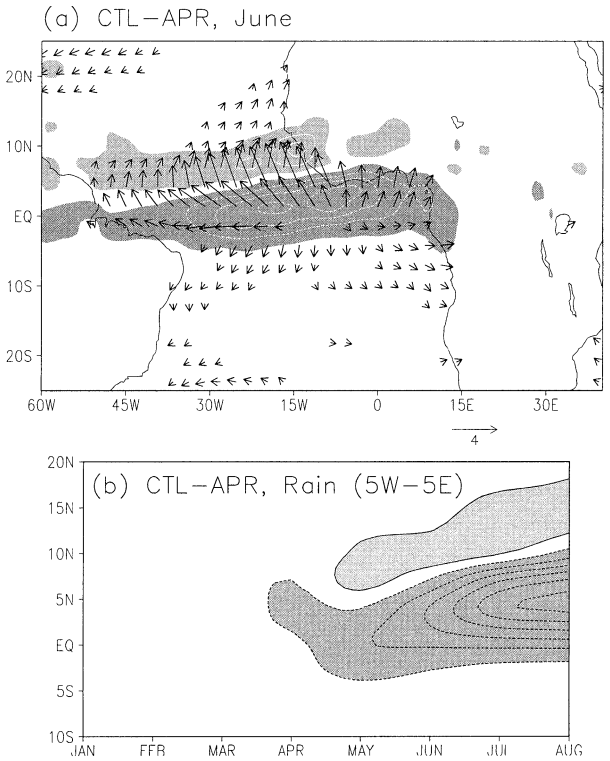

FIG. 6. (a) CTL − APR anomalies of precipitation (light shade > 1.0 mm day^{-1} and dark shade < −1.0 mm day^{-1} with white contours at intervals of 2.0 mm day^{-1}) and surface wind (vectors; m s^{-1}) in Jun. (b) Latitude–time section of CTL − APR precipitation anomalies averaged in 5.0°W–5.0°E. Shading and contour intervals are the same as in (a).

In the ANM run, where the equatorial Atlantic SST is held to its annual-mean value, the African monsoon onset is as abrupt as in the CTL run over the Gulf of Guinea (Fig. 5c), in agreement with Li and Philander (1997). This difference between the APR and ANM runs suggests that the monsoon–cold tongue interaction is nonlinear. As long as SST in the Gulf of Guinea is cool enough to suppress deep convection there, the African monsoon starts abruptly even without the help of further cooling in the equatorial Atlantic (the ANM run). In reality, however, the equatorial SST cools down from its March–April peak below the convective threshold in response to the southerly monsoon over the Gulf of Guinea. It in turn helps accelerate the development of the African monsoon and pushes the rainband inland away from the coast, suggesting the interactive nature between the monsoon and equatorial cold tongue. The rest of the paper investigates the mechanisms for atmospheric transition from the warm to cold season by contrasting the model results with and without the seasonal development of the equatorial cold tongue. While interesting in its own right, we will not discuss the ANM run further since in the warm season (March–April) the equatorial Atlantic is too cold (Fig. 2a) and the simulated atmospheric state is too far away from that in the CTL run.

b. Effect on equatorial cooling

This section considers how the surface wind changes cause the equatorial cooling from spring to summer. For

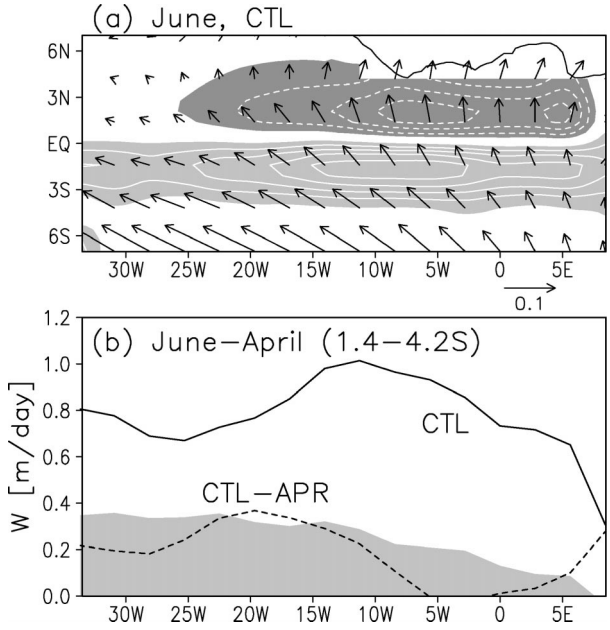

FIG. 7. (a) Ekman pumping velocity (light shade > 0.5 m day^{-1} and dark shade < -0.5 m day^{-1} with white contours at intervals of 0.5 m day^{-1}; positive value means upwelling) and surface wind stress (vectors; N m^{-2}) in Jun in the CTL run. (b) Jun − Apr changes in Ekman pumping velocity (m day^{-1}) averaged south of the equator (1.4°–4.2°S) for the CTL run (solid) and CTL − APR anomalies (dashed). Shading denotes the contribution from zonal wind stress in the CTL run.

simplicity, we limit ourselves to a qualitative discussion and consider only the wind-induced changes in upwelling and thermocline depth. The wind-induced adjustments in the surface heat flux and the relative contributions to the equatorial cooling among all these factors require a more sophisticated ocean model to be properly assessed and are left for future studies.

The observed Atlantic cold tongue is centered slightly south of the equator, indicative of upwelling induced by the cross-equatorial southerlies. Ekman pumping velocity is calculated from the surface wind stresses in the CTL and APR runs based on a frictional Ekman model as outlined in the appendix. In April, even before the monsoon onset, weak cross-equatorial southerlies exist over the central/eastern basin, and the cold subsurface water upwells to the surface south of the equator (not shown). With the onset of the African monsoon, the upwelling velocity nearly triples from April to June. The maximum velocity reaches as large as 2.5 m day^{-1} over the eastern/central basin in June (Fig. 7a).

In the eastern equatorial Atlantic, the enhanced cross-equatorial southerlies are the major cause of the large increase in the upwelling velocity from April to June, with the easterly winds also making a significant contribution (10%–20%; compare the solid line and shading in Fig. 7b). [This ratio may be model dependent given that this AGCM tends to simulate too strongly an annual cycle of equatorial zonal winds (Fig. 4).] The upwelling velocity there hardly changes in the APR run without the seasonal cooling on the equator (dashed line in Fig. 7b). Comparing the CTL and APR runs, we note that in the eastern basin, the anomalous surface winds induced by the equatorial cooling do not cross the equator but diverge away from it (Fig. 6a). While these divergent winds would induce a small upwelling near the equator [Eq. (A4)], it is offset by the downwelling induced by the weak westerly anomalies in the east. The strong southerly winds over the Gulf of Guinea, however, may contribute to the further equatorial cooling by increasing vertical mixing and evaporation.

In the western basin, the easterly winds become more important, forcing 30%–50% of the seasonal upwelling. The equatorial cooling that takes place from April to June induces strong anomalous easterlies in the western half of the equatorial basin (Fig. 6a), which further induces upwelling cooling near the equator. The CTL − APR difference indicates that this interaction between the equatorial easterlies and SST contributes to 30%–50% of the seasonal upwelling in the western basin (dashed line in Fig. 7b). This is probably a lower limit of the easterly wind effect on equatorial seasonal cooling since these winds would force the thermocline to shoal in the eastern basin via equatorial Kelvin waves, intensifying the upwelling cooling there. This nonlocal effect of equatorial easterly winds has been noted previously (Adamec and O'Brien 1978; Moore et al. 1978; McCreary et al. 1984). Indeed, observational studies show that the eastern Atlantic thermocline shoals by 40 m in summer and significantly contributes to the seasonal cooling in the east (Houghton 1983; Weisberg and Colin 1986).

To assess the importance of these SST-induced zonal winds in the seasonal thermocline displacement, we force a linear reduced-gravity model with daily surface wind stresses simulated in the CTL and APR runs. The model follows Zebiak and Cane (1987) and Zebiak (1993) and solves the time evolution of the thermocline depth. Figure 8 shows the changes in the thermocline depth along the equator from 1 April to 30 July. We chose this period because the SST-induced equatorial zonal winds are largest in July instead of June (Fig. 9b). Induced by the eastern ocean cooling in the CTL run, enhanced equatorial easterly winds over the central/western basin shoal the thermocline in the east and deepen in the west with a node around 20°W (solid line in Fig. 8). Without strong easterly acceleration in the APR run, the thermocline shoaling is only half of that in the case with the CTL run's wind stress (dashed line in Fig. 8). Thus, equatorial easterly winds, accelerated at the western edge of the cold tongue, may feed back significantly to the eastern ocean cooling by shoaling the thermocline and reducing the subsurface temperature there.

5. Seasonal cycle of the equatorial zonal wind

Thus, zonal winds are an important forcing for the seasonal upwelling and thermocline displacement in the

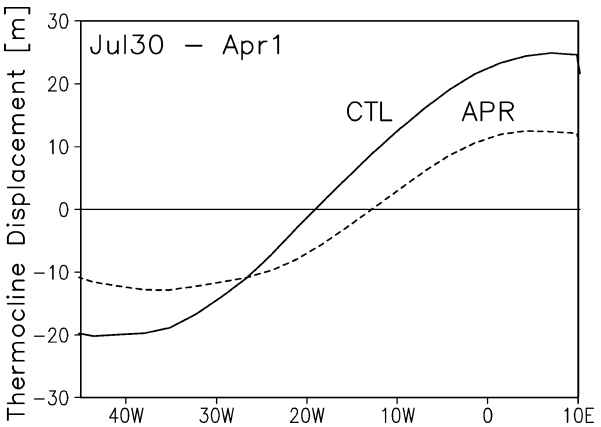

FIG. 8. Thermocline displacement (shoaling; m) along the equator (0.5°S–0.5°N) from 1 Apr to 30 Jul in the linear reduced-gravity model forced with surface wind stresses simulated in the CTL (solid) and APR (dashed) runs.

equatorial Atlantic. This section investigates the mechanisms for the seasonal variations in the equatorial zonal wind. Figure 9a shows the deviation of zonal wind velocity from its annual mean along the equator as a function of longitude and calendar month in the CTL run, together with CTL − APR SST anomalies. Anomalous easterly (westerly) winds first appear in the east in summer (spring) and then propagate westward. The SST anomalies show a weaker but somewhat similar westward propagation along the equator.

a. SST gradient effect

Nearly all the intensification of equatorial easterly winds west of 20°W in the CTL run is due to the cold tongue development and attendant SST gradient. In the APR run with the cold tongue removed, the zonal winds in the western equatorial Atlantic remain nearly steady from 15 April onward (Fig. 9b), consistent with previous studies suggesting that the interaction of equatorial zonal wind and SST is the cause of their covariations. The SST-induced zonal wind exceeds 4 m s^{-1} in the central equatorial Atlantic in July, which has a great impact on the zonal tilt of the equatorial thermocline and its shoaling in the east as demonstrated in the last section. This SST effect on zonal wind is different from Li and Philander's (1997) result that seasonal variations in SST are unimportant for the annual cycle of zonal wind over the western equatorial Atlantic (their Fig. 2). This difference in sensitivity to equatorial SST may result from model differences, but we note that sampling size in their analysis may also be partially responsible; the simulated equatorial winds in their model display considerable subseasonal variability. They compare the simulated seasonal cycle at one single grid point in the western basin while our analysis is based on a 10-yr average and includes the full zonal dimension.

In the eastern equatorial Atlantic, the annual cycle of the zonal wind is very similar in the CTL and APR runs (Fig. 9). West of 10°W, the development of anomalous easterlies in summer is surprisingly well simulated in the APR run without the equatorial cooling. A question remains: what causes these seasonal changes in the equatorial zonal wind in the absence of any changes in the zonal SST gradient? The rest of this section addresses this issue.

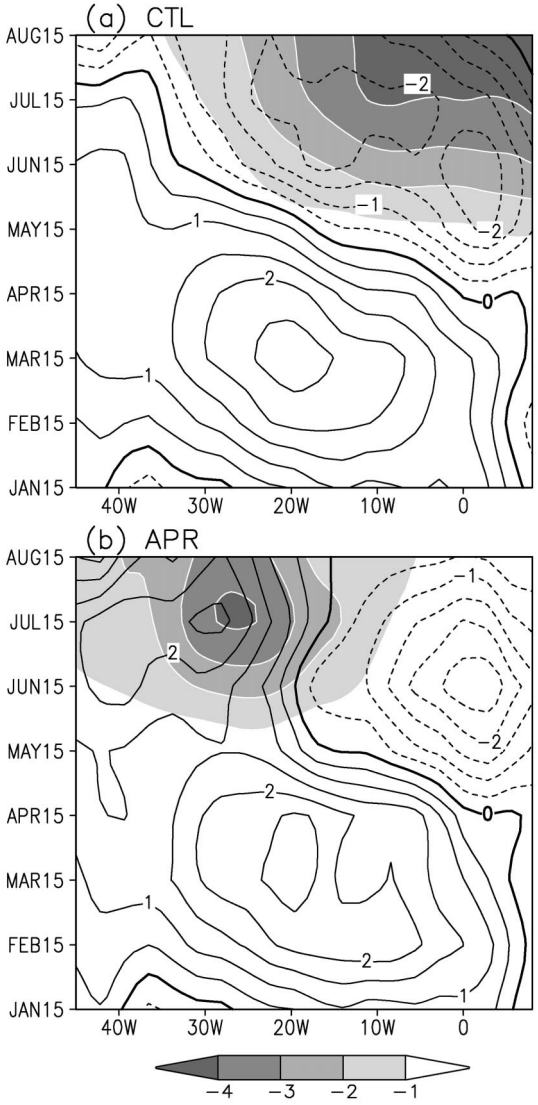

FIG. 9. Seasonal cycle of surface zonal winds (m s^{-1}) along the equator (1.4°N–1.4°S) in the (a) CTL and (b) APR runs. Contour intervals are 0.5 m s^{-1}. In both (a) and (b), the annual mean value in the CTL run is subtracted. Shading shows the CTL − APR anomalies in (a) SST and (b) surface zonal wind (scale for both shading is shown in the bottom).

b. Monsoon heating distribution

The African continent is asymmetric about the equator, and the seasonal variations in continental rainfall

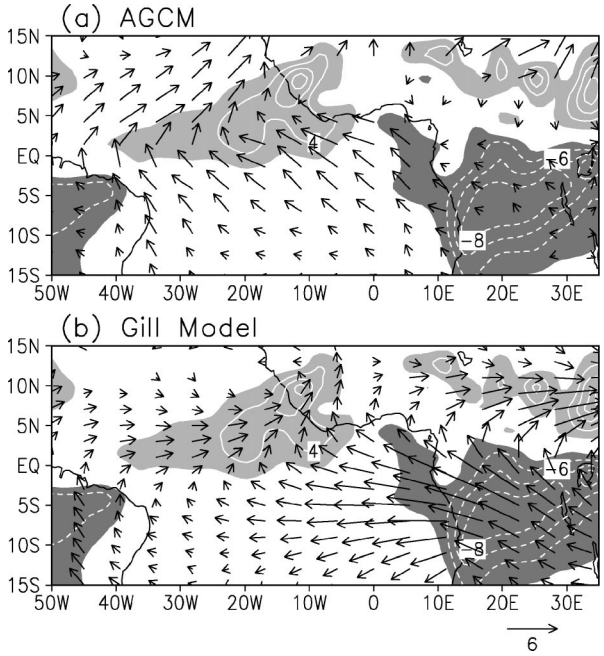

FIG. 10. (a) Same as in Fig. 3a, but for changes in the APR run. (b) Surface wind response (vectors; m s^{-1}) to this precipitation change (redrawn) in the linear model.

may lead to changes in equatorial wind. In the June − April precipitation difference field for the APR run (Fig. 10a), the negative heating over central Africa is much greater south than north of the equator. This negative heating over central Africa and the positive heating associated with the oceanic ITCZ to the west would likely induce zonal pressure gradients that drive equatorial easterlies south of Guinea. To demonstrate the effect of this zonal displacement of major negative and positive heating centers of the monsoon, we force a linear baroclinic model of the atmosphere with the June − April heating anomalies in Fig. 10a, following Matsuno (1966) and Gill (1980). This simple model reproduces the equatorial easterlies in the eastern Atlantic (Fig. 10b) as part of the Rossby response to the negative heating over central Africa. We note that this model is useful only in a qualitative sense since the magnitude of its response is sensitive to the choice of the damping rate, which is set constant in space.

c. Equatorward momentum advection

The linear model with a resting background state does not explain the easterly anomalies in the June − April difference field for the APR run in the western equatorial Atlantic (Fig. 10), which turns out to be due to the equatorward advection of the easterly momentum. By integrating the zonal momentum equation through the boundary layer, the zonal momentum equation near the equator may be written approximately as

$$\varepsilon u = -\frac{1}{\rho}\frac{\partial P}{\partial x} - v\frac{\partial u}{\partial y} + fv, \tag{2}$$

where the vertical eddy viscosity is parameterized as a simple damping term with a time scale of ε^{-1}. All the other variables have their conventional meanings. We have neglected the zonal advection since the wind variations are much greater in the cross-equatorial than in the zonal direction. The vertical advection is also omitted in light of reduced shear at the top of the planetary boundary layer. Subtracting the annual mean leads to the following equation for the seasonal deviation of zonal wind velocity:

$$\varepsilon u' = -\frac{1}{\rho}\frac{\partial P'}{\partial x} - \left[v'\frac{\partial \overline{u}}{\partial y} + \overline{v}\frac{\partial u'}{\partial y} + \left(v'\frac{\partial u'}{\partial y} - \overline{v'\frac{\partial u'}{\partial y}}\right)\right] + fv', \tag{3}$$

where the overbar and prime denote the annual mean and seasonal deviation, respectively.

With the climatological ITCZ displaced north of the equator, time-averaged winds are southerlies ($\overline{v} > 0$) at the equator. The Coriolis force acting upon these southerlies accelerates the easterly winds south of the equator and decelerates them to the north, giving rise to a northward shear of the zonal wind near the equator ($\partial\overline{u}/\partial y > 0$). As the African monsoon intensifies from April to June, the cross-equatorial southerly winds strengthen ($v' > 0$) and so does the northward gradient of zonal winds ($\partial u'/\partial y > 0$). Thus, the first three terms in the brackets of Eq. (3) are positive, and this northward advection of the easterly momentum acts to accelerate the easterly winds on the equator. This momentum advection term is particularly effective in varying the zonal wind near the equator where it cannot be balanced by the vanishing Coriolis force.

d. Momentum balance

Figure 11 shows the longitude–time sections of the terms on the right-hand side of Eq. (2) in the GCM and COADS observations. In both the model and observations, the sum of these terms is highly correlated with the annual cycle of the equatorial zonal wind velocity, indicating that Eq. (2) is indeed a good approximation of the momentum balance in the boundary layer. In the APR run, both the African monsoon–induced pressure gradient and momentum advection contribute to the easterly acceleration in summer over the eastern Atlantic. The effect of the former is limited to east of 5°W, consistent with the linear model result (Fig. 10), and the momentum advection is solely responsible for the easterly anomalies to the west in June relative to April in the APR run.

While the terms in the momentum budget are quite similar both in pattern and magnitude between the CTL

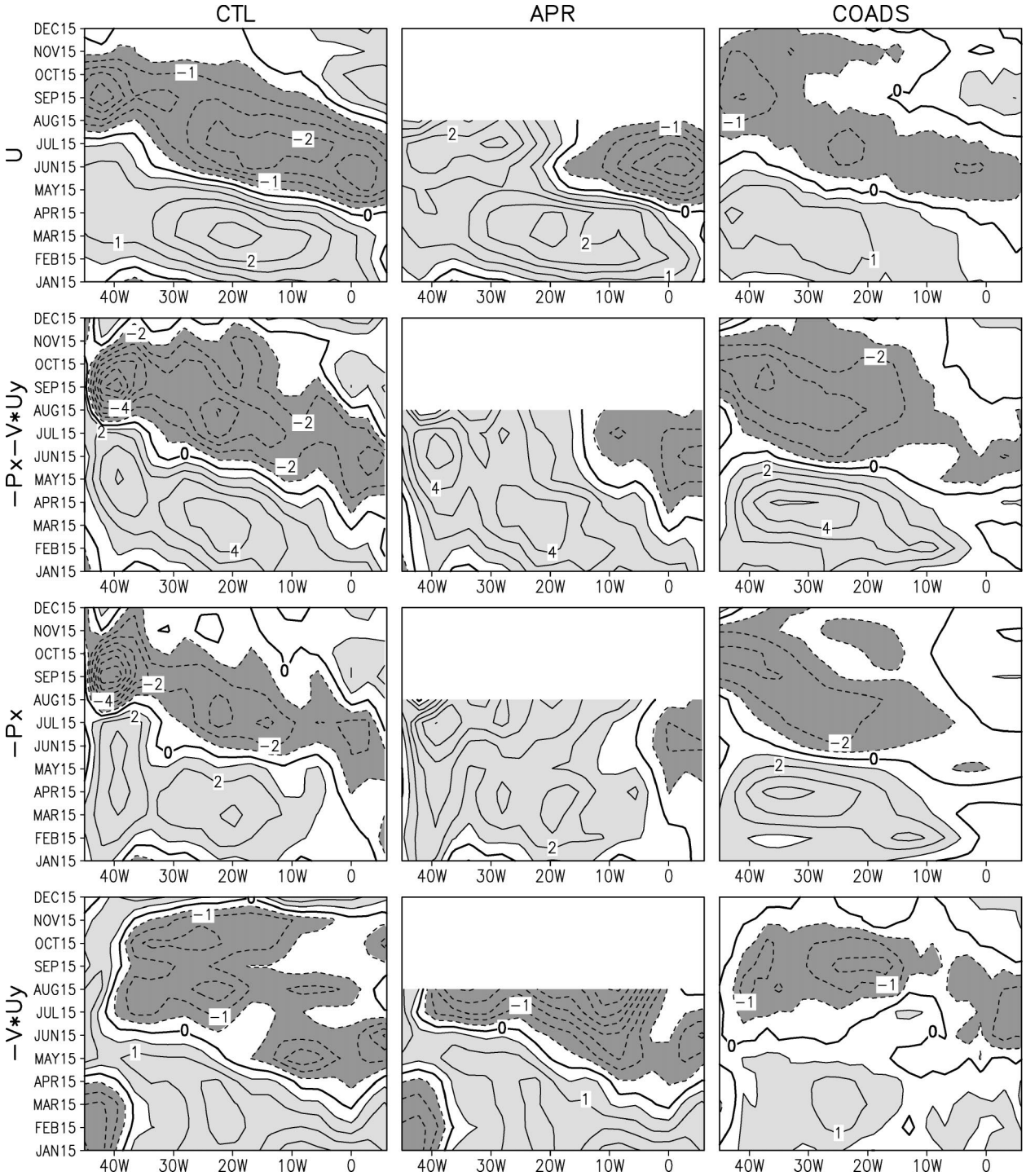

FIG. 11. (first row) Seasonal cycle of equatorial surface zonal wind (m s^{-1}) and zonal momentum acceleration by (third row) pressure gradient force (10^{-5} m s^{-2}), (fourth row) meridional advection (10^{-5} m s^{-2}), and (second row) their sum (10^{-5} m s^{-2}) in the (left) CTL and (middle) APR runs and (right) COADS climatology. Annual mean values are subtracted in each panel. (In the column for the APR run, those in the CTL run are subtracted.) From the top row, contour intervals are 0.5 m s^{-1}, 1.0, 1.0, and 0.5 $\times$ 10^{-5} m s^{-2}. Values smaller (greater) than the first negative (positive) contour are shaded with light (dark) gray.

run and observations, the wind annual cycle in the CTL run is a factor of 2 too strong, suggesting that the momentum dissipation is too weak in the model. The pressure gradient now accounts for two-thirds of the easterly acceleration in summer in the CTL run (cf. the middle panels in the left column of Fig. 11), reaffirming the effect of equatorial SST annual cycle on sea level pressure and winds. This SST effect on winds is particularly large west of 5°W. In the CTL run, the momentum advection is roughly the same as in the APR run east of 5°W but is considerably reduced in magnitude over the rest of the equatorial Atlantic because the SST-induced zonal winds (Fig. 6a) act to weaken the positive wind shear in the meridional direction; namely, $\partial u'/\partial y$ is smaller near the equator in the CTL run. Because of this SST effect on the wind shear, the APR run overestimates the easterly acceleration due to meridional momentum advection. Or equivalently, the CTL − APR differencing analysis underestimates the SST effect on the annual cycle of equatorial zonal winds.

The pressure gradient term shows a clear westward propagation, in support of the notion that it results from the interaction of equatorial SST and zonal winds. Rather unexpected, however, is an apparent westward propagation in the momentum advection term, which is particularly pronounced in the GCM in the first half of the year. This results from the different timing of the monsoon onsets in the eastern and western Atlantic. The early onset of the African summer monsoon in May causes the cross-equatorial southerly winds to surge and advect easterly momentum from the south into the equator. The southerly phase in the western equatorial Atlantic takes place two months later than in the east and peaks in September, as in the rest of the global oceanic monsoon (e.g., in the equatorial Pacific). Over the ocean, the maximum meridional SST gradient occurs in August–September because of its great thermal inertia. West Africa, by contrast, heats up rapidly as the sun moves into the Northern Hemisphere, causing the rapid acceleration of the cross-equatorial southerlies in the eastern equatorial Atlantic.

6. Summary and discussion

We have conducted a series of AGCM experiments that are designed to investigate the role of air–sea interaction in the equatorial Atlantic annual cycle. Our results show that the seasonal development of the equatorial cold tongue contributes significantly to the abrupt onset of the southerly monsoon in the Gulf of Guinea and to the northward advance of the monsoon rainband on West Africa. The monsoon, in turn, exerts a strong influence on the seasonal evolution of the equatorial cold tongue, through cross-equatorial southeasterly winds. Consistent with Mitchell and Wallace (1992), the interaction of equatorial SST and zonal winds is very important for their westward copropagation.

Our results suggest the following conceptual model for the seasonal evolution of the African monsoon–cold tongue complex. After the spring equinox, solar radiation quickly heats up the West African continent and establishes a strong northward gradient of surface temperature. In the atmospheric boundary layer, the resultant pressure gradient accelerates the southerly winds over the Gulf of Guinea. These cross-equatorial southerlies induce oceanic upwelling south of the equator that cools the eastern equatorial Atlantic. The equatorial cooling intensifies the southerly monsoon in the Gulf of Guinea and pushes the continental rainband inland from the Guinean coast. The northward shift of the continental/oceanic rainband generates an eastward pressure gradient that drives easterly winds in the eastern equatorial Atlantic. Across the equatorial Atlantic, the intensified southerlies advect the easterly momentum from the south into the equator and this advective effect explains about one-third of the easterly acceleration. In response to the onset of the African monsoon, the upwelling cooling is strongest in the east both because of the strong acceleration of the southerly winds and because the thermocline is shallow there. This eastern cooling establishes an eastward surface pressure gradient that accelerates the easterly winds in the middle and western equatorial Atlantic. This interaction of equatorial SST and zonal winds helps to spread the eastern cooling westward over the rest of the equatorial Atlantic.

Three mechanisms for summer easterly wind acceleration over the equatorial Atlantic are identified: the zonal SST gradient mechanism is important in the middle and western Atlantic; the effect of pressure gradients induced by monsoon heating distribution outside the equatorial Atlantic is limited to the eastern Atlantic south of West Africa; and the equatorward momentum advection is a significant contributor across the basin. The accelerated easterlies contribute to the equatorial cooling by inducing upwelling and by shoaling the thermocline in the east.

The effect of seasonal equatorial ocean cooling on West African summer precipitation as demonstrated here is consistent with previous studies of interannual variability associated with the Atlantic Niño (e.g., Lamb 1978; Hastenrath 1984; Lough 1986; Janowiak 1988; Wagner and da Silva 1993). The Atlantic ITCZ and precipitation over the surrounding continents vary also with another mode of SST variability that is characterized by a strong cross-equatorial SST gradient (Nobre and Shukla 1996; Okumura et al. 2001). Air–sea interaction within the tropical Atlantic, along with external forcing such as the El Niño–Southern Oscillation and North Atlantic Oscillation, is important for developing both the equatorial mode and the meridional gradient mode (Chang et al. 1997; Xie and Tanimoto 1998; Huang et al. 2002; see Xie and Carton 2004 for a recent review of tropical Atlantic variability).

As in the tropical Pacific, much of the tropical Atlantic climate variability appears to be a modification

in its annual cycle (Hastenrath 1984). However, the coupled aspect of the equatorial Atlantic annual cycle is not as well understood as its Pacific counterpart and many state-of-the-art coupled GCMs have difficulty in simulating the realistic climatology and annual cycle in the tropical Atlantic (Davey et al. 2002), which has been shown to strongly affect the spatiotemporal structure of interannual variability (Okajima et al. 2003).

Of a relatively small zonal width, the Atlantic climate is strongly influenced by its surrounding continents. Indeed, our results show that the onset of the African monsoon triggers the seasonal development of the equatorial cold tongue in the Atlantic. When ocean and atmospheric models are coupled, small errors can be amplified through their interaction. A realistic representation of the air–sea–land interaction is necessary for a realistic simulation of the mean state and interannual variability of the tropical Atlantic climate in coupled models.

Acknowledgments. The authors would like to thank the anonymous reviewers for useful comments. This study is supported by the NOAA CLIVAR Atlantic program, CCSR at University of Tokyo, and the Frontier Research System for Global Change.

APPENDIX

Ekman Pumping Velocity

The governing equations for surface current velocity in a frictional Ekman model (Zebiak and Cane 1987) are

$$r_s u_s - \beta_0 y v_s = \frac{\tau_x}{\rho_o H} \quad \text{and} \tag{A1}$$

$$r_s v_s + \beta_0 y u_s = \frac{\tau_y}{\rho_o H}, \tag{A2}$$

where the subscript s denotes the shear between the surface and the depth of the Ekman/mixed layer H, $r_s = (2 \text{ days})^{-1}$ is the friction coefficient for the shear current, $\beta_0 y$ is the Coriolis parameter on an equatorial beta plane, and τ is the surface wind stress. The other variables have the conventional meaning. The upwelling velocity w_s at the depth H is calculated as

$$w_s = H[(u_s)_x + (v_s)_y]. \tag{A3}$$

Equation (A3) can be rewritten in terms of wind stresses as

$$w_s = \frac{1}{\rho_o(\beta_0^2 y^2 + r_s^2)}\left\{\frac{\beta_0}{\beta_0^2 y^2 + r_s^2}[(\beta_0^2 y^2 - r_s^2)\tau_x - 2\beta_0 y r_s \tau_y] + r_s \nabla \cdot \boldsymbol{\tau} + \beta_0 y \nabla \times \boldsymbol{\tau}\right\}. \tag{A4}$$

In the vicinity of the equator ($y \approx 0$), easterly winds ($\tau_x < 0$) effectively bring subsurface cold water upward as the first term on the right-hand side becomes positive. Slightly off the equator, the second term becomes more important, and cross-equatorial southerlies ($\tau_y > 0$) induce upwelling (downwelling) to the south (north) of the equator. Besides wind stresses themselves, their divergence and curl can also contribute to oceanic upwelling (the last two terms). Sufficiently away from the equator, the wind curl effect becomes dominant.

REFERENCES

Adamec, D., and J. J. O'Brien, 1978: The seasonal upwelling in the Gulf of Guinea due to remote forcing. *J. Phys. Oceanogr.*, **8,** 1050–1060.

Chang, P., 1996: The role of the dynamic ocean–atmosphere interactions in the tropical seasonal cycle. *J. Climate,* **9,** 2973–2985.

——, L. Ji, and H. Li, 1997: A decadal climate variation in the tropical Atlantic Ocean from thermodynamic air–sea interactions. *Nature,* **385,** 516–518.

Davey, M. K., and Coauthors, 2002: STOIC: A study of coupled model climatology and variability in tropical ocean regions. *Climate Dyn.,* **18,** 403–420.

Eltahir, E. A. B., and C. Gong, 1996: Dynamics of wet and dry years in West Africa. *J. Climate,* **9,** 1030–1042.

Fontaine, B., S. Janicot, and P. Roucou, 1999: Coupled ocean–atmosphere surface variability and its climate impacts in the tropical Atlantic region. *Climate Dyn.,* **15,** 451–473.

Gates, W. L., and Coauthors, 1999: An overview of the results of the Atmospheric Model Intercomparison Project (AMIP I). *Bull. Amer. Meteor. Soc.,* **80,** 29–55.

Gill, A. E., 1980: Some simple solutions for heat-induced tropical circulation. *Quart. J. Roy. Meteor. Soc.,* **106,** 447–462.

Hastenrath, S., 1984: Interannual variability and annual cycle: Mechanisms of circulation and climate in the tropical Atlantic sector. *Mon. Wea. Rev.,* **112,** 1097–1107.

Houghton, R. W., 1983: Seasonal variations of the subsurface thermal structure in the Gulf of Guinea. *J. Phys. Oceanogr.,* **13,** 2070–2081.

Huang, B., P. S. Schopf, and Z. Pan, 2002: The ENSO effect on the tropical Atlantic variability. *Geophys. Res. Lett.,* **29,** 2039, doi:10.1029/2002GL014872.

Janicot, S., A. Harzallah, B. Fontaine, and V. Moron, 1998: West African monsoon dynamics and eastern equatorial Atlantic and Pacific SST anomalies (1979–88). *J. Climate,* **11,** 1847–1882.

Janowiak, J. E., 1988: An investigation of interannual rainfall variability in Africa. *J. Climate,* **1,** 240–255.

Kalnay, E., and Coauthors, 1996: The NCEP/NCAR 40-Year Reanalysis Project. *Bull. Amer. Meteor. Soc.,* **77,** 437–471.

Lamb, P. J., 1978: Case studies of tropical Atlantic surface circulation patterns during recent sub-Saharan weather anomalies: 1967 and 1968. *Mon. Wea. Rev.,* **106,** 482–491.

Li, T., and S. G. H. Philander, 1997: On the seasonal cycle of the equatorial Atlantic Ocean. *J. Climate,* **10,** 813–817.

Lough, J. M., 1986: Tropical Atlantic sea surface temperatures and rainfall variations in sub-Saharan Africa. *Mon. Wea. Rev.,* **114,** 561–570.

Matsuno, T., 1966: Quasi-geostrophic motions in the equatorial area. *J. Meteor. Soc. Japan,* **44,** 25–43.

McCreary, J., J. Picaut, and D. Moore, 1984: Effects of the remote annual forcing in the eastern tropical Atlantic Ocean. *J. Mar. Res.,* **42,** 45–81.

Mitchell, T., and J. M. Wallace, 1992: The annual cycle in equatorial convection and sea surface temperature. *J. Climate,* **5,** 1140–1156.

Moore, D., P. Hisard, J. P. McCreary, J. Merlo, J. J. O'Brien, J. Picaut,

J. M. Verstraete, and C. Wunsch, 1978: Equatorial adjustment in the eastern Atlantic. *Geophys. Res. Lett.,* **8,** 637–640.

Nigam, S., and Y. Chao, 1996: Evolution dynamics of tropical ocean–atmosphere annual cycle variability. *J. Climate,* **9,** 3187–3205.

Nobre, P., and J. Shukla, 1996: Variations of sea surface temperature, wind stress, and rainfall over the tropical Atlantic and South America. *J. Climate,* **9,** 2464–2479.

Numaguti, A., 1999: Origin and recycling processes of precipitating water over the Eurasian continent: Experiments using an atmospheric general circulation model. *J. Geophys. Res.,* **104,** 1957–1972.

——, M. Takahashi, T. Nakajima, and A. Sumi, 1995: Development of an atmospheric general circulation model. *Climate System Dynamics and Modeling,* T. Matsuno, Ed., Center for Climate System Research, University of Tokyo, 1–27. [Available from CCSR, University of Tokyo, 4-6-1 Komaba, Meguro, Tokyo 153-8904, Japan.]

Okajima, H., S.-P. Xie, and A. Numaguti, 2003: Interhemispheric coherence of tropical climate variability: Effect of the climatological ITCZ. *J. Meteor. Soc. Japan,* **81,** 1371–1386.

Okumura, Y., S.-P. Xie, A. Numaguti, and Y. Tanimoto, 2001: Tropical Atlantic air–sea interaction and its influence on the NAO. *Geophys. Res. Lett.,* **28,** 1507–1510.

Philander, S. G. H., and R. C. Pacanowski, 1981: The oceanic response to cross-equatorial winds (with application to coastal upwelling in low latitudes). *Tellus,* **33,** 201–210.

——, D. Gu, D. Halpern, G. Lambert, N.-C. Lau, T. Li, and R. C. Pacanowski, 1996: Why the ITCZ is mostly north of the equator. *J. Climate,* **9,** 2958–2972.

Sultan, B., and S. Janicot, 2003: The West African monsoon dynamics. Part II: The ''preonset'' and ''onset'' of the summer monsoon. *J. Climate,* **16,** 3407–3427.

Wagner, R. G., and A. M. da Silva, 1994: Surface conditions associated with anomalous rainfall in the Guinea coastal region. *Int. J. Climatol.,* **14,** 179–199.

Ward, M. N., 1998: Diagnosis and short-lead time prediction of summer rainfall in tropical North Africa at interannual and multidecadal timescales. *J. Climate,* **11,** 3167–3191.

Weisberg, R. H., and C. Colin, 1986: Equatorial Atlantic Ocean temperature and current variations during 1983 and 1984. *Nature,* **322,** 240–243.

Xie, P., and P. A. Arkin, 1996: Analyses of global monthly precipitation using gauge observations, satellite estimates, and numerical model predictions. *J. Climate,* **9,** 840–858.

Xie, S.-P., 1994: On the genesis of the equatorial annual cycle. *J. Climate,* **7,** 2008–2013.

——, 2004: The shape of continents, air–sea interaction, and the rising branch of the Hadley circulation. *The Hadley Circulation: Past, Present and Future,* H. F. Diaz and R. S. Bradley, Eds., Kluwer Academic.

——, and Y. Tanimoto, 1998: A pan-Atlantic decadal climate oscillation. *Geophys. Res. Lett.,* **25,** 2185–2188.

——, and J. A. Carton, 2004: Tropical Atlantic variability: Patterns, mechanisms, and impacts. *Earth Climate: The Ocean–Atmosphere Interaction, Geophys. Monogr.,* Amer. Geophys. Union, 121–141.

Zebiak, S. E., 1993: Air–sea interaction in the equatorial Atlantic region. *J. Climate,* **6,** 1567–1586.

——, and M. A. Cane, 1987: A model El Niño–Southern Oscillation. *Mon. Wea. Rev.,* **115,** 2262–2278.